Eds. (Chapman Hall, New York, 1993), pp. 384–401.
21. L. Keller and K. G. Ross, *Science* **260**, 1107 (1993).
22. To determine primary sex ratios, approximately 50 eggs (a small fraction of the total number of eggs) were collected at the onset of egg laying, between late April and mid-May, when sexual brood is produced [K. Gösswald, *Die Waldameise Vol. 1* (AULA-Verlag, Wiesbaden, Germany, 1989)]. The number of chromosomes ($2n$ = 52) [E. Hauschteck-Jungen, and H. Jungen, *Insect Soc.* **23**, 513 (1976)] was assessed (*11*) (blind with respect to colony identity and queen mating frequency) in at least 5 but usually 10 cells per egg. The large number of chromosomes sometimes precluded counts of all chromosomes, so eggs in which fewer than 26 chromosomes were consistently found were classified as males, whereas those with more than 40 chromosomes were classified as females. Only nests with at least 20 successfully sexed eggs were included in the analyses, so that two nests in 1994 and three in 1995 were discarded.
23. We made efforts to collect eggs immediately after the onset of egg laying in April/May, when only sexual brood is laid. However, worker-destined eggs are laid from mid-May onward, causing a slight overlap in worker and sexual brood, so a few worker-destined eggs may have been included in the primary sex ratio sample. Hence, the primary sex ratios obtained here may slightly overestimate the proportion of females among the eggs, and consequently provide a conservative test of differences in primary and secondary sex ratios in the singly mated class. The sample sizes differ from those given in Table 1, because three colonies that were scored for primary sex ratios only produced worker brood in 1994.
24. We thank J. J. Boomsma, A. F. G. Bourke, W. D. Brown, E. A. Herre, M. Milinski, D. Nash, T. Reuter, F. L. W. Ratnieks, P. Sherman, and three anonymous referees for comments on the manuscript; C. Chang, R. Forsman, P. Gertsch, A.-M. Mehmeti, I. Schmidt, and H. Åberg for assistance; and Tvärminne Zoological Station in Finland for working facilities. The study was funded by the Academy of Finland; Svenska Kulturfonden; Société Vaudoise des Sciences Naturelles; Swiss National Science Foundation; and Fondation du 450e anniversaire, University of Lausanne.

1 July 1996; accepted 13 September 1996

Hypertension Induced in Pregnant Mice by Placental Renin and Maternal Angiotensinogen

Eriko Takimoto, Junji Ishida, Fumihiro Sugiyama, Hisashi Horiguchi, Kazuo Murakami, Akiyoshi Fukamizu*

Maternal hypertension is a common complication of pregnancy and its pathophysiology is poorly understood. This phenomenon was studied in an animal model by mating transgenic mice expressing components of the human renin-angiotensin system. When transgenic females expressing angiotensinogen were mated with transgenic males expressing renin, the pregnant females displayed a transient elevation of blood pressure in late pregnancy, due to secretion of placental human renin into the maternal circulation. Blood pressure returned to normal levels after delivery of the pups. Histopathologic examination revealed uniform enlargement of glomeruli associated with an increase in urinary protein excretion, myocardial hypertrophy, and necrosis and edema in the placenta. These mice may provide molecular insights into pregnancy-associated hypertension in humans.

Pregnancy induces extensive maternal adaptations in cardiovascular and renal physiology. Circulating levels of renin and angiotensin, proteins that serve as primary regulators of blood pressure and body-fluid volume, markedly increase during pregnancy (*1*). Although alterations of the renin-angiotensin system have long been suspected to contribute to pregnancy-associated hypertension (*2*, *3*), the pathogenesis of this hypertension is not clear. The presence of renin in the placenta indicates that there is local renin synthesis (*4*) and suggests the possible involvement of renin in the regulation of maternal blood pressure and uteroplacental vascular resistance and blood flow (*5*). However, there is no direct in vivo evidence that renin is secreted from the placenta into the maternal circulation or that a paternally derived factor contributes to the regulation of maternal blood pressure.

We have created lines of transgenic mice carrying either the human renin gene (*6*) or the human angiotensinogen gene (*7*). These mice were normotensive despite the normal tissue-specific expression pattern of transgenes, but the F_1 progeny expressing both human genes exhibited a chronic hypertension (*8*). During the cross-mating experiments, we observed that transgenic female mice carrying the human angiotensinogen gene, which displayed normal blood pressure in the nonpregnant state, developed hypertension at 19 days of gestation, but only when they had been mated with transgenic males carrying the human renin gene (Table 1). Pregnant females derived from other mating combinations did not show hypertension. On the basis of these results, we hypothesized that the combined action of placental renin and maternal angiotensinogen might play a role in the development of pregnancy-associated hypertension.

To test this hypothesis, we conducted a time-course measurement of blood pressure elevation during pregnancy. The blood pressure of the human-angiotensinogen transgenic females mated with the human-renin transgenic males began to increase at 14 days of gestation, continued to rise until the day before delivery, and returned to the level seen in the nonpregnant state by 3 days after delivery (Fig. 1A). In contrast, control mice did not show any change in blood pressure throughout pregnancy.

To examine whether renin derived from male mice carrying the human renin gene is secreted into the maternal circulation, we measured plasma human renin

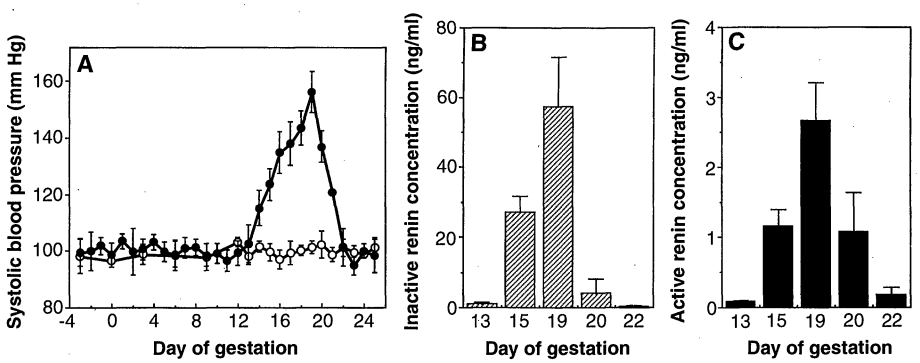

Fig. 1. Systolic blood pressure and human renin concentration in the murine maternal circulation before and during pregnancy, and after delivery. Day 0 is the day of coitus. (**A**) Changes in systolic blood pressure of pregnant mice. Results are expressed as means ± SD for each determination (*14*). Day 20 was the day of delivery and systolic blood pressure was measured afterward. (●) hRN male × hANG female (n = 18 mice); (○) WT × WT (n = 7 mice). Changes in inactive (**B**) and active (**C**) human renin concentration in the maternal circulation of pregnant mice with hypertension. Values are the means ± SD. Four animals were used for each determination by radioimmunoassay (*15*).

E. Takimoto, J. Ishida, K. Murakami, A. Fukamizu, Institute of Applied Biochemistry and Tsukuba Advanced Research Alliance (TARA), University of Tsukuba, Ibaraki 305, Japan.
F. Sugiyama, Laboratory Animal Research Center, University of Tsukuba, Ibaraki 305, Japan.
H. Horiguchi, Institute of Basic Medical Sciences, University of Tsukuba, Ibaraki 305, Japan.
*To whom correspondence should be addressed. E-mail: akif@sakura.cc.tsukuba.ac.jp

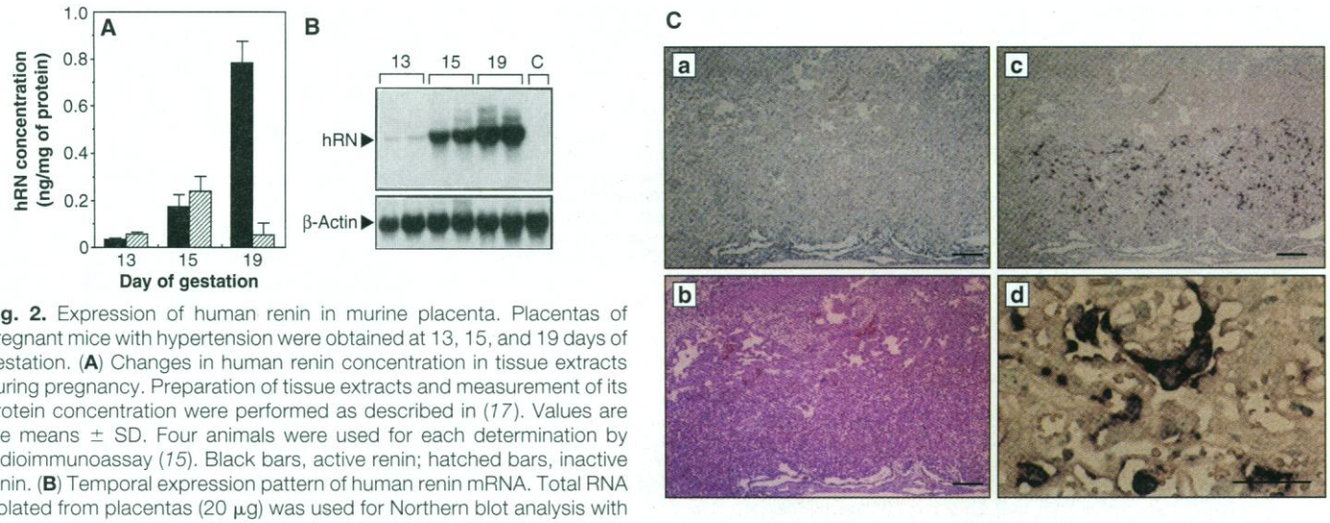

Fig. 2. Expression of human renin in murine placenta. Placentas of pregnant mice with hypertension were obtained at 13, 15, and 19 days of gestation. (**A**) Changes in human renin concentration in tissue extracts during pregnancy. Preparation of tissue extracts and measurement of its protein concentration were performed as described in (*17*). Values are the means ± SD. Four animals were used for each determination by radioimmunoassay (*15*). Black bars, active renin; hatched bars, inactive renin. (**B**) Temporal expression pattern of human renin mRNA. Total RNA isolated from placentas (20 μg) was used for Northern blot analysis with probes for human renin (hRN) (*13*) and β-actin (*18*). The number indicates the day of gestation. Placenta at 19 days of gestation of wild-type mice (WT) mated with WT male mice were used as a negative control (lane labeled C). (**C**) Localization of human renin mRNA determined by in situ hybridization as described in (*19*). Placentas at 19 days of gestation were hybridized with the sense (panel a) or antisense (panels c and d) human renin digoxigenin-labeled probe, or stained histochemically with hematoxylin and eosin (panel b) according to standard procedures. Scale bars in panels a, b, and c, 200 μm; in panel d, 50 μm.

concentrations. The levels of both prorenin and active renin increased from 13 days of gestation (Fig. 1, B and C). In humans, plasma levels of prorenin and active renin have been shown to rise during pregnancy (9), and it has been postulated that placentally derived renin may contribute to this rise (*10*). We therefore measured human renin concentrations and human renin mRNA accumulation in the murine placenta. The level of human active renin in the placental tissue extracts of the pregnant mice gradually increased throughout pregnancy (Fig. 2A, black bars) as did the accumulation of human renin mRNA (Fig. 2B). We also examined the production site of human renin in the placenta of pregnant wild-type female mice mated with human-renin transgenic males by in situ hybridization at 19 days of gestation (Fig. 2C). Hybridization signals were localized to chorionic trophoblasts, consistent with previous observations on human placenta (*4*). In addition, treatment of the transgenic hypertensive females with ES-8891, an inhibitor specific for human renin (*8*, *11*), at 17 days of gestation significantly reduced blood pressure (Table 2). These results demonstrate that late in pregnancy, the placental human renin is secreted into the maternal circulation.

We also observed morphological abnormalities in the transgenic hypertensive mice late in pregnancy. On histologic examination, the glomeruli were uniformly

Table 1. Comparison of systolic blood pressure in pregnant mice. Systolic blood pressure at 19 days of gestation was measured by the tailcuff method as described in (*14*). Values are the means and standard deviations. A statistically significant elevation was observed only when transgenic (hANG) females had been mated with transgenic (hRN) males. hRN, transgenic mice carrying the human renin gene; hANG, transgenic mice carrying the human angiotensinogen gene; WT, wild-type mice; *n*, numbers of mice.

Mating combination ♂	× ♀	Systolic blood pressure (mm Hg)	*n*
hRN	hANG	156.4 ± 7.73*	8
hANG	hRN	95.5 ± 5.59	8
hRN	WT	96.7 ± 4.01	4
hANG	WT	98.7 ± 3.66	4
WT	hRN	90.9 ± 1.75	4
WT	hANG	101.3 ± 6.18	4
WT	WT	100.0 ± 3.14	6

*P = 0.0001, by Student's t test.

Table 2. Comparison of parameters between mice with pregnancy-associated hypertension and normotensive control mice. Human renin and angiotensin II levels in plasma at 19 days of gestation were measured by radioimmunoassay (*15*). Changes in systolic blood pressure before and after 1 hour of oral administration of ES-8891 (60 mg per kilogram of body weight) (*8*, *11*) at 17 days of gestation are shown. Urine collection at 19 days of gestation and measurement of total urinary protein was performed as in (*16*). The ratio of heart weight to body weight was measured in the same tissues for histopathological examinations. All values represented are means and standard deviations. Student's t test was used to compare the two groups. Statistical significance of effect of ES-8891 was determined by the Wilcoxon signed-rank test. *n*, Numbers of mice; b.w., body weight; N.D., not detectable; –, not done.

Parameter	Mating combination ♂ hRN × ♀ hANG	*n*	♂ hRN × ♀ WT	*n*	♂ WT × ♀ WT	*n*
Human renin						
Active (ng/ml)	2.66 ± 0.54*	4	1.61 ± 0.13	5	N.D.	
Inactive (ng/ml)	57.43 ± 14.29	4	54.12 ± 3.57	5	N.D.	
Angiotensin II (pg/ml)	465.36 ± 85.04*	5	85.64 ± 19.62	5	75.41 ± 28.74	5
Effect of ES-8891						
Before (mm Hg)	136.71 ± 3.22	6	–		96.73 ± 4.01	6
After (mm Hg)	116.93 ± 2.73**	6	–		96.76 ± 5.21	6
Water intake (ml/day per 10 g of b.w.)	6.93 ± 0.07*	3	–		2.30 ± 0.46	3
Urine volume (ml/day per 10 g of b.w.)	3.90 ± 0.62***	3	–		0.79 ± 0.36	3
Urinary protein excretion (mg/day per 10 g of b.w.)	11.99 ± 0.45*	3	–		1.76 ± 0.63	3
Ratio of heart weight to body weight (mg/g)	9.97 ± 0.73*	5	–		4.33 ± 0.57	5

*P = 0.0001. **P = 0.0022. ***P = 0.0017.

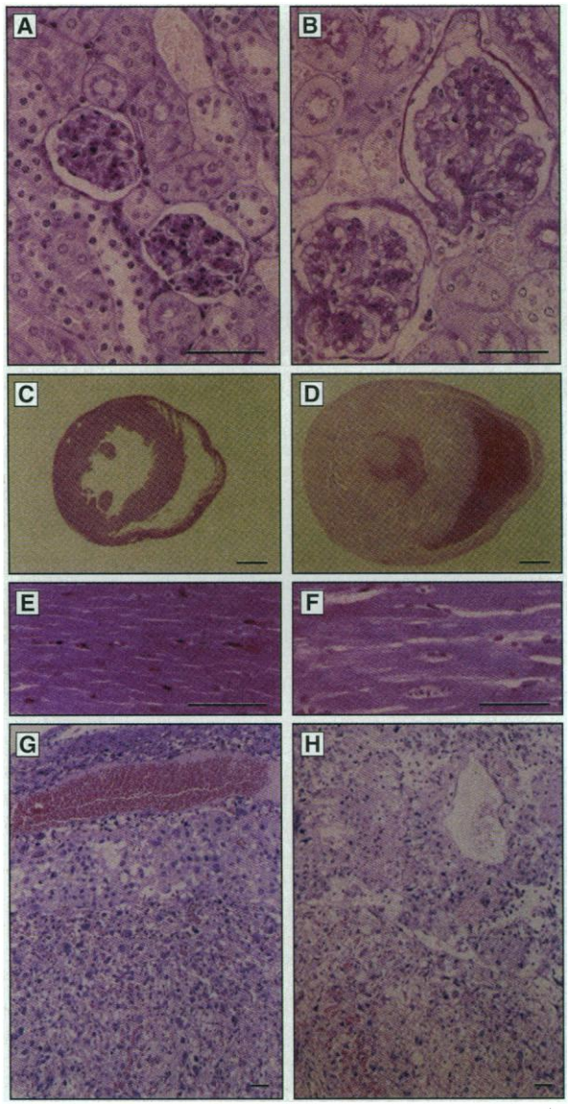

Fig. 3. Histopathological analysis (*20*) of mice with pregnancy-associated hypertension. Tissues of hypertensive pregnant mice that had died or were killed at 16 to 20 days of gestation were obtained. As a control, tissues were obtained from gestational age-matched wild-type pregnant mice. In contrast to a control (**A**), the kidney in a hypertensive pregnant mouse (**B**) shows uniform enlargement of glomeruli. In contrast to a control (**C**), a cross section of the heart of a hypertensive pregnant mouse (**D**) shows myocardial concentric hypertrophy. In contrast to a control (**E**), a hypertensive pregnant mouse shows the left ventricle uniformly thickening because of typical muscular hypertrophy (**F**). In contrast to a control (**G**), the placenta in a hypertensive pregnant mouse shows necrosis in spongiotrophoblasts and decidua cells, edematous enlargement, and congestion in chorion cells (**H**). Scale bars in (A), (B), and (E) through (H), 50 μm; in (C) and (D), 1 mm.

enlarged (Fig. 3B), and this was associated with an increase in urinary protein excretion (Table 2). Autopsy revealed myocardial concentric hypertrophy (Fig. 3, D and F) in all of the transgenic hypertensive mice and intrathoracic or intra-abdominal hemorrhage in 23% (6/26) of them. The heart weight-to-body weight ratio in these mice was two times that in the control mice at late gestation (Table 2). Consequently, only 38% (10/26) of the transgenic mice with hypertension survived throughout pregnancy. Furthermore, delivery was delayed in all of the hypertensive pregnant mice that survived. Generalized convulsions occurred in 15% (4/26) of the hypertensive pregnant mice late in pregnancy, and one of the four also had intra-abdominal hemorrhage.

Autopsy also revealed necrosis in spongiotrophoblasts and decidua cells, edematous enlargement, and congestion in chorion cells in the hypertensive pregnant mice (Fig. 3H). In women with pregnancy-associated hypertension, the concentration of active renin in the placenta is significantly higher than that of normal pregnant women, which may be a response to the decrease in uteroplacental blood flow (*2*). The impaired blood flow may be due to the loss of refractoriness of the uteroplacental vasculature or to the effect of high levels of circulating angiotensin II (*12*). Indeed, in comparison to normotensive pregnant mice, hypertensive pregnant mice had elevated plasma levels of angiotensin II and active renin (Table 2), which probably reflects human renin production in the placenta. It is thus possible that the combined action of placental renin and maternal angiotensinogen in the peripheral uteroplacental circulation could also induce hypertension in the transgenic pregnant females.

We have presented evidence that a paternally derived factor produced in the placenta is secreted into the maternal circulation. In principle, this type of transgenic approach is applicable not only to pregnancy-associated hypertension, but to any disease that is induced by the combination of fetal and maternal factors. The mice described here may be useful for the molecular dissection of the pathophysiology underlying pregnancy-associated hypertension and may lead to new treatments for this disorder.

REFERENCES AND NOTES

1. S. L. Skinner, *The Renin-Angiotensin System* (Gower Medical, London, 1993), pp. 50.1–50.16.
2. H. S. Brar *et al.*, *Am. J. Obstet. Gynecol.* **157**, 363 (1987).
3. S. W. Graves, E. W. Seely, G. H. Williams, *Nature Genet.* **4**, 7 (1993); K. Ward *et al.*, *ibid.*, p. 59; R. Arngrimsson *et al.*, *ibid.*, p. 114.
4. E. M. Symonds, M. A. Stanley, S. L. Skinner, *Nature* **217**, 1152 (1968); A. Y. Warren, D. J. Craven, E. M. Symonds, *Br. J. Obstet. Gynaecol.* **89**, 628 (1982); K. J. Shaw *et al.*, *J. Clin. Invest.* **83**, 2085 (1989); Y. Ihara, S. Taii, T. Mori, *Endocrinol. Jpn.* **34**, 887 (1987).
5. A. Hagemann, A. H. Nielsen, K. Poulsen, *Exp. Clin. Endocrinol.* **102**, 252 (1994).
6. A. Fukamizu *et al.*, *Biochem. Biophys. Res. Commun.* **165**, 826 (1989).
7. S. Takahashi *et al.*, *ibid.* **180**, 1103 (1991).
8. A. Fukamizu *et al.*, *J. Biol. Chem.* **268**, 11617 (1993).
9. M. Wilson *et al.*, *Am. J. Med.* **68**, 97 (1980); W. A. Hsueh *et al.*, *J. Clin. Endocrinol. Metab.* **54**, 1010 (1982); J. E. Sealey *et al.*, *Am. J. Obstet. Gynecol.* **153**, 514 (1985).
10. T. Lenz, G. D. James, J. H. Laragh, J. E. Sealey, *Am. J. Physiol.* **260**, E876 (1991).
11. Y. Ii, E. Murakami, K. Hiwada, *J. Hypertens.* **9**, 1119 (1991).
12. R. P. Naden and C. R. Rosenfeld, *J. Clin. Invest.* **68**, 468 (1981).
13. T. Imai *et al.*, *Proc. Natl. Acad. Sci. U.S.A.* **80**, 7405 (1983).
14. The systolic blood pressure of pregnant mice was measured by a programmable sphygmomanometer (BP-98; Sftron, Japan) by using the tailcuff method [K. Tanimoto *et al.*, *J. Biol. Chem.* **269**, 31334 (1994)]. Transgenic mice and age-matched wild-type mice (C57BL/6J) at 2 to 4 months were used for cross-mating.
15. Human active renin concentration was measured by direct radioimmunoassay (*8*). Total renin concentration was defined as the renin concentration measured after prorenin activation by trypsin (Sigma) [T. Lenz, J. E. Sealey, P. August, G. D. James, J. H. Laragh, *J. Clin. Endocrinol. Metab.* **69**, 31 (1989)]. Inactive renin concentration was calculated as the difference between active and total renin concentration. Mouse renin did not cross-react with the human monoclonal antibodies used in this assay.
16. All animals were placed in individual metabolic cages (CLEA Japan Inc.) with free access to food and water. After an adaptation period of 1 week, 24-hour urine samples were collected. Total urinary protein concentration was measured by the protein assay kit (Bio-Rad). Transgenic mice and wild-type mice at 4 months of age were used for cross-mating.
17. A. Fukamizu *et al.*, *Drug Res.* **43(I)**, 222 (1993).
18. K. Tokunaga, H. Taniguchi, K. Yoda, M. Shimizu, S. Sakiyama, *Nucleic Acids Res.* **14**, 2829 (1986).
19. Placentas of wild-type mice mated with male mice carrying the human renin gene were fixed in 4% paraformaldehyde, embedded in paraffin, and cut into 3-μm serial sections. Sections were deparaffinized and hybridized with a digoxigenin-labeled probe, synthesized as sense and antisense RNAs from the Aat II–Sac I 405–base pair fragment of the human renin cDNA (*13*) in the presence of digoxigenin-labeled uridine-triphosphate (Boehringer Mann-

heim). After the color reaction, the sections were counter stained with methyl green.
20. Tissues of pregnant mice were fixed in 10% buffered formalin and embedded in paraffin. Deparaffinized tissue sections were stained with hematoxylin and eosin, and other reagents such as periodic acid-Schiff and Masson trichrome if necessary.
21. We thank the Laboratory Animal Research Center at the University of Tsukuba and T. Watanabe and T. Mori for their technical advice and assistance. Care of experimental animals was within institutional guidelines. Supported by grants from the Ministry of Education, Science, Sports and Culture of Japan, and Circulation Biosystems at the University of Tsukuba. E.T. and J.I. are research fellows of the Japan Society for the Promotion of Science.

22 April 1996; accepted 5 September 1996

Laser Capture Microdissection

Michael R. Emmert-Buck, Robert F. Bonner, Paul D. Smith, Rodrigo F. Chuaqui, Zhengping Zhuang, Seth R. Goldstein, Rhonda A. Weiss, Lance A. Liotta*

Laser capture microdissection (LCM) under direct microscopic visualization permits rapid one-step procurement of selected human cell populations from a section of complex, heterogeneous tissue. In this technique, a transparent thermoplastic film (ethylene vinyl acetate polymer) is applied to the surface of the tissue section on a standard glass histopathology slide; a carbon dioxide laser pulse then specifically activates the film above the cells of interest. Strong focal adhesion allows selective procurement of the targeted cells. Multiple examples of LCM transfer and tissue analysis, including polymerase chain reaction amplification of DNA and RNA, and enzyme recovery from transferred tissue are demonstrated.

As basic research links more and more genes to the cause of, predisposition for, or clinical behavior of specific diseases, the medical diagnostic laboratory will be transformed. Clinical molecular diagnostic testing will involve the measurement of simultaneous fluctuations of expression of multiple genes or genetic alterations occurring in developing or diseased tissues; thus, the next generation of molecular analysis methods will need to be miniaturized and automated. Several groups have proposed the development of image chips or array systems containing thousands of sequences for automated hybridization (*1*, *2*). Each chip can simultaneously assay for several possible genetic mutations or measure the relative expression of multiple mRNA species (*3*). Alternatively, a serial analysis of gene expression (SAGE) approach can be used to simultaneously assess mRNA expression of multiple transcripts (*4*). With the use of polymerase chain reaction (PCR) amplification and such automated technology, molecular diagnostic testing in the future will likely consist of panels of tests rather than a few single tests for specific genes. In this way, a specific genetic fingerprint will be established for each individual lesion, which will be useful for diagnosis and prognosis and as a guide to therapy.

However, even the most sophisticated genetic testing methods will be of limited value if the input DNA, RNA, or proteins are not derived from pure populations of cells exhibiting the characteristic disease morphology. Several methods have been reported for tissue microdissection to address the problems associated with analysis of heterogeneous tissue. These include gross dissection of frozen tissue blocks to enrich for specific cell populations (*5*, *6*), irradiation of manually ink-stained sections to destroy unwanted genetic material (*7*), touch preparations of frozen tissue specimens (*8*), and microdissection with manual tools (*9*–*12*). However, none of these methods offers the ease, precision, and efficiency necessary for routine research or clinical molecular diagnostic applications. For example, although manual microdissection can achieve good precision, it is time-consuming, labor-intensive, and requires a high degree of manual dexterity.

To overcome the drawbacks of current tissue microdissection techniques, we have developed a laser capture microdissection (LCM) system (Fig. 1). The method entails placing a thin transparent film over a tissue section, visualizing the tissue microscopically, and selectively adhering the cells of interest to the film with a fixed-position, short-duration, focused pulse from an infrared laser. The film with the procured tissue is then removed from the section and placed directly into DNA, RNA, or enzyme buffer for processing.

LCM has several advantages over current tissue microdissection approaches: It is simple, requires no moving parts, involves no manual microdissection or manipulations, and enables one-step transfers. The transferred tissue on the film retains its original morphology, thereby allowing microscopic verification of the specificity of the captured material. LCM can be performed almost as quickly as photography of histologic tissue sections. The use of sterile, disposable transfer films minimizes potential contamination, which is particularly important for PCR-based analyses. The films can be activated with minimal energy; small, inexpensive low-power lasers (<50 mW) that can be attached to standard microscopes are sufficient. LCM has the potential to fulfill the critical needs of basic researchers and clinicians to perform tissue microdissection on a routine basis.

The selective transfer and recovery of human tissue samples by LCM is shown in Fig. 2 (*13*, *14*). These images represent the transfer of kidney glomeruli, Alzheimer's plaques in brain, in situ breast carcinoma, atypical ductal hyperplasia (ADH) of the breast, prostatic intraepithelial neoplasia (PIN), and lymphoid follicles. We have found no limitations on the types of tissue samples that can be procured by LCM and

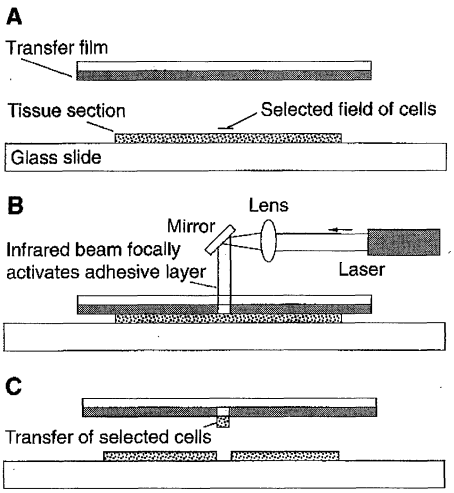

Fig. 1. (**A**) Transparent EVA thermoplastic film is applied to the surface of a routine tissue section mounted on a glass slide. The tissue–EVA film sandwich is viewed under a microscope, and the cells of interest are positioned in the center of the field. (**B**) A focused laser beam coaxial with the microscope optics is pulsed to activate the film, causing it to become focally adhesive and fuse to the selected underlying cells in the tissue section. (**C**) When the EVA film is removed from the tissue section, the selected cells remain adherent to the film surface. The film is then placed directly into the DNA, RNA, or enzyme buffer. The cellular material detaches from the film and is ready for standard processing.

M. R. Emmert-Buck, R. F. Chuaqui, Z. Zhuang, R. A. Weiss, L. A. Liotta, Laboratory of Pathology, National Cancer Institute, Room 2A33, Building 10, 9000 Rockville Pike, Bethesda, MD 20892, USA.
R. F. Bonner, P. D. Smith, S. R. Goldstein, Biomedical Engineering and Instrumentation Program, National Center for Research Resources, National Institutes of Health, Bethesda, MD 20892, USA.
*To whom correspondence should be addressed.